

## Adaptive Finite-element Analysis of Plastic Deformation of Plates under Projectile Impact

T. Prakash, G.S. Sekhon and N.K. Gupta  
 Indian Institute of Technology Delhi, New Delhi-110 016

### ABSTRACT

This paper deals with the finite-element analysis of plastic deformation of plates during normal impact of projectile on plates. The finite element method implemented here is based on the flow formulation of plasticity. During projectile impact the geometrical configuration of domain is progressively altered that generally causes distortion of mesh. It affects the accuracy of finite-element solution. Hence, *a posteriori* error estimation for the computed finite-element solution has been incorporated to capture the zones of high stress and strain gradients. The *h*-refinement of the mesh is carried out over such domain to limit the solution error. Two projectile impact problems on a circular aluminium plate—one by a blunt-end projectile and another by a hemi-spherical-headed projectile—are analysed to illustrate the proposed method.

**Keywords:** Finite-element analysis, aluminium plates, plastic deformation, projectile impact, closed-form solutions, plasticity, metal plates, flow formulation

### NOMENCLATURE

$\sigma'_{ij}$	Deviatoric stress
$\bar{\sigma}$	Effective stress
$\dot{\epsilon}_{ij}$	Strain rate
$\dot{\bar{\epsilon}}$	Effective strain rate
$\epsilon_v$	Volumetric strain rate
$F$	Applied force
$\Omega$	Domain of the problem
$\Gamma_f$	Boundary surface where $F$ is defined
$\eta_{allow}$	Prescribed error percentage

$\ e\ $	Energy norm
$e_u$	Error in displacement field
$e_\sigma$	Error in stress field

### 1. INTRODUCTION

Impact and impact-related problems have attracted considerable research interest over the past few decades. Substantial efforts have been made in understanding the physics of the phenomena during ordnance ballistic penetration and to model these mathematically. Remarkable progress has been made in experimental investigations of the normal perforation of metal plates, as revealed by literature study. However, due to the complexity and cost involved in ballistic experiments, it is not optimal to base all impact-related studies on laboratory tests alone.

Therefore, analytical and numerical solution techniques are needed as a supplement to high-precision testing to reduce the experimental needs to a minimum.

A number of analytical models have been proposed over the years, but the complexity of many impact events often limits the general use of closed-form analytical solutions. It is often imperative to use numerical methods to solve this class of problems. However, numerical studies involving impact and penetration in the sub-ordnance and ordnance velocity regime are still few in the published literature, mainly due to the scarcity of reliable material description and fracture modelling during perforation. With the advent of computers, finite-element method is evolving into a powerful numerical tool to solve a variety of structural problems. The recent development of adaptive finite-element procedures has made the finite-element method more reliable and robust. The present work is a contribution to the finite-element simulation of the projectile impact on plates in the adaptive setting.

Backman and Goldsmith<sup>1</sup> described aspects of terminal ballistics and discussed penetration mechanics caused by different kinds of penetrators and targets and the influence of projectile and target parameters that affect the penetration phenomenon. Levy and Goldsmith<sup>2</sup> presented experimental results on forces, permanent deflections, strains, and plugs produced by rigid projectiles. Aluminium and mild steel plates were impacted with projectiles whose velocity ranged from 20 m/s to 300 m/s. Three nose shapes, viz., blunt, spherical, and conical were fitted to the instrumented projectile body. Projectiles of diameters 6.35 mm and 12.7 mm were employed.

Liss and Goldsmith<sup>3</sup> investigated normal impact of both the rigid and the deformable blunt cylinders against soft (2024-0) aluminium plates of varying thicknesses over a velocity range of 60 m/s to 600 m/s. Speeds just below and well above the ballistic limit (the minimum velocity required to perforate the target completely through the thickness direction) were used.

Kobayashi<sup>4</sup>, *et al.* suggested a visco-plastic behaviour of material for incorporating rate-dependency

effects. An approach to achieve a satisfactory formulation for time-dependent behaviour has been to generalise plasticity for cases within the strain rate sensitivity range. One such formulation has been provided by the theory of visco-plasticity.

The problem of over-constraint due to incompressibility of the plastic deformation has been examined by many authors. An approach called selective reduced integration method was suggested by Zienkiewicz<sup>5</sup>, *et al.* Later, Coupez and Chenot<sup>6</sup> examined the classical conditions of enforcing incompressibility by means of the penalty method.

Zienkiewicz and Zhu<sup>7</sup> proposed an easy to implement error estimator in the existing finite-element codes. The estimator allows estimation of both the global and the local errors. It can be combined with an adaptive process of refinement that allows the user to obtain desired accuracy.

A general recovery technique has been developed by Zienkiewicz and Zhu<sup>8</sup> for determining the derivatives (stresses) of a finite-element solution at the nodes. The technique has been tested on a group of linear, quadratic, and cubic elements for both one- and two-dimensional problems.

Singh<sup>9</sup> developed a code for meshing a 2-D domain using advancing wavefront technique. A finite-element program, Form2d has been written for the simulation of forming operations. It works in an adaptive setting.

## 2. FINITE-ELEMENT FORMULATION

During impact, the target material is subjected to larger strain, strain rates and temperature. Hence, the material is assumed to behave as a rigid plastic or rigid visco-plastic material. The flow formulation<sup>4</sup> may be adopted to arrive at the finite-element equations. It requires that among admissible velocities,  $u_i$  that satisfies the conditions of compatibility and incompressibility, as well as the velocity boundary conditions, the actual solution gives the following functional, (function of functions) a stationary value.

$$\pi = \int_{\Omega} \sigma'_{ij} \dot{\epsilon}_{ij} d\Omega - \int_{\Gamma_f} F_i u_i d\Gamma_f \quad (1)$$

Expressing Eqn (1) in terms of equivalent stress, equivalent strain and imposing the incompressibility constraint by introducing the penalised, the following relationship is obtained.

$$\delta\pi = \int_{\Omega} \bar{\sigma} \delta \bar{\epsilon} d\Omega + K \int_{\Omega} \bar{\epsilon}_v \delta \bar{\epsilon}_v d\Omega - \int_{\Gamma_f} F_j \delta u_j d\Gamma_f \quad (2)$$

where  $K$  is a large positive constant. Discretising the domain  $\Omega$  and minimising the functional gives the following relation.

$$\left[ \frac{\partial \pi}{\partial v_i} \right]_{v=v_0} + \left[ \frac{\partial^2 \pi}{\partial v_i \partial v_j} \right]_{v=v_0} \Delta v_j = 0 \quad (3)$$

On simplifying the above, one obtains the following matrix equation

$$K \Delta v = f \quad (4)$$

where  $K$  is the stiffness matrix and  $f$  is the residual of the nodal point force vector whose expressions are given as

$$K = \frac{\partial^2 \pi}{\partial v_i \partial v_j} = \int_{\Omega} \bar{\epsilon} P_{ij} d\Omega + \int_{\Omega} \left( \frac{1}{\bar{\epsilon}} \frac{\partial \bar{\sigma}}{\partial \bar{\epsilon}} - \frac{\bar{\sigma}}{\bar{\epsilon}^2} \right) \frac{1}{\bar{\epsilon}} P_{ij} v_k v_m P_{mj} d\Omega + \int_{\Omega} K C_j C_i d\Omega \quad (5)$$

$$f = \frac{\partial \pi}{\partial v_j} = \int_{\Omega} \bar{\sigma} P_{ij} V_j d\Omega + \int_{\Omega} K C_j V_j C_i d\Omega - \int_{\Gamma_f} F_j N_{ji} d\Gamma_f \quad (6)$$

where  $\left( \frac{\partial \bar{\sigma}}{\partial \bar{\epsilon}} \right) = v^T P v$ ;  $P = B^T D B$ ;  $C_i = B_{1i} + B_{2i} + B_{3i}$ ;  $B$  is strain rate matrix;  $D$  is constitutive matrix and  $v$  is nodal velocity vector.

Solving Eqn (4), the velocity correction term is obtained. Subsequently, the approximate velocity  $v_0$  is corrected as

$$v = v_0 + \Delta v \quad (7)$$

The nodal velocity is determined when convergence is achieved.

### 3. ERROR ESTIMATION & ADAPTIVE REFINEMENT

During impact, the configuration of the domain is progressively altered, causing increasing distortion of elements, that can lead to increase in the error of FEM solution. Hence, *a posteriori* error estimation of the computed solution becomes essential to assess the accuracy of the analysis. The approximate finite-element solution expressed in terms of computed displacement  $u^h$  and stress  $\sigma^h$ , differs from the corresponding exact solution expressed by  $u$  and  $\sigma$ . As the exact solution to the problem obviously is not known *a priori*, an improved solution ( $u^*, \sigma^*$ ) is obtained by a so-called recovery procedure<sup>8</sup>. The point-wise error is estimated in terms of deviations as

$$e^*_{\sigma} = \sigma^* - \sigma^h \quad (8)$$

$$e^*_{u} = u^* - u^h \quad (9)$$

The point-wise definitions of errors are generally difficult to specify and the elemental error measures are quantified by computing the strain energy which is the difference between the discontinuous finite-element solution and the smoothed solution<sup>7</sup>.

$$|e_i|^2 = \int_{\Omega_i} (\sigma^{*h} - \sigma^h)^T (\bar{\epsilon} - \bar{\epsilon}^h) d\Omega \quad (10)$$

Global strain energy error measure is given by

$|e|^2 = \sum_{i=1}^n |e_i|^2$ , where  $n$  is the total number of elements. The global error measure can be normalised in terms of total energy in the system as follows

$$\eta = \frac{|e|}{\left( |U^h|^2 + |e|^2 \right)^{1/2}} \times 100\% \quad (11)$$

where  $U^h$  is the total energy dissipation contained in the finite-element solution given by  $|U^h|^2 = \sum_{i=2}^n |U_i^h|^2$  and  $|U^h|^2 = \int_{\Omega} \sigma^h \bar{\epsilon} d\Omega$ . The solution is acceptable

if  $\eta \leq \eta_{allow}$  where  $\eta_{allow}$  is the prescribed percentage. If not,  $h$ -refinement is carried out by implementing the following procedure.

Permissible global error is given by  $|e|_{allow} = \frac{\eta_{allow}|e|}{k}$ , where  $k$  is a factor lying between 1.0 to 1.5 to prevent oscillations. The permissible elemental error for the  $i^{th}$  element is given by the relation

$|e|_{allow(i)} = \frac{|e|_{allow}}{\sqrt{N}}$  (by distributing the error equally over all elements of the domain) where  $N$  is the total number of elements in the domain. Alternatively,

one can make  $|e|_{allow(i)} = |e|_{allow} \left( \frac{\Omega_i}{\Omega} \right)^{1/2}$  where  $\Omega$  is the volume of the domain,  $\Omega_i$  is the volume of the  $i^{th}$  element. This strategy is called distributing square of error equally among elements. Then, element refinement parameter is calculated using the relation

$|e|_{allow(i)} = \frac{|e|_i}{|e|_{allow(i)}}$ . Finally, the new element size is determined from the previous element size  $h_{new} = \frac{h_{old}}{\xi_i^{1/p}}$ .

With this new element size evaluated at the nodes, the mesh is regenerated adaptively according to the error in the finite-element solution.

#### 4. ANALYSIS

Two problems, namely permanent deformation of an axisymmetric thin plate subjected to impact by a spherical-head projectile, and by a blunt-end projectile, were chosen for illustrating the proposed finite-element procedure.

##### 4.1 Impact of a Blunt-end Projectile on an Axisymmetric Metallic Target

A finite-element analysis under adaptive environment is performed to simulate the large deformation of a circular aluminum plate during impact by a blunt-end projectile. Due to the rotational symmetry, only the sectional plane is considered as the problem domain. This plane is discretised using six-noded triangular elements. The target is a plate of thickness 3.2 mm and diameter 120 mm. The different input parameters are as follows: Projectile velocity = 86.8 m/s

Projectile mass = 39.8 g

Projectile diameter = 12.5 mm

Time step  $\Delta t = 5 \mu s$

Specific heat capacity = 875 J/kg

Mass density of the target material = 2780 kg/m<sup>3</sup>

The relation between effective stress and effective strain used for the simulation<sup>3</sup> is given as

$\bar{\sigma} = 165 + 850\bar{\epsilon}$  where  $\bar{\sigma}$  is effective stress and  $\bar{\epsilon}$  is effective strain<sup>3</sup>.  $\eta_u$ (upper error limit) = 11 per cent,  $\eta_a$ (aiming error) = 10 per cent. The deformation of the plate at various time steps is plotted in Fig. 1.

The deflected profile of the plate along the radial distance is shown in Fig. 2. The maximum deflection of the plate is 13.7 mm. It approximately matches<sup>3</sup> with the experimental value of 14.2 mm.

Error in energy norm is plotted for different time steps. Whenever the error exceeds the limit  $\eta_u$ , the mesh is regenerated. Initially, the error is around 15.5 per cent for the discretised domain of 541 elements and 1165 nodes. Afterwards, the mesh is regenerated to have 599 elements and 1346 nodes and the error is below  $\eta_u$  upto 31<sup>st</sup> step, and once again, it initially exceeds the limit and then is suppressed by the mesh regeneration which discretise the domain into 282 elements and 647 nodes. Similarly, two more regenerations are carried out in the few next steps. It can be seen that the mesh regeneration is automatically performed whenever error exceeds the limit. Thus, the three peaks shown in the plot Fig. 4 are suppressed by the adaptive mesh regeneration.

From Fig. 1 two regions in the plate appear to have more number of fine elements. One of these is located near the tip of the projectile and the other around the holder. It is observed that the mesh gets progressively refined in regions where the strain and strain rates are high. This shows the effectiveness of the error estimation and adaptive mesh refinement. Also, coarser elements are generated where the strain gradient are not very high. This restricts the total number of elements in the mesh and helps reduce computational time.

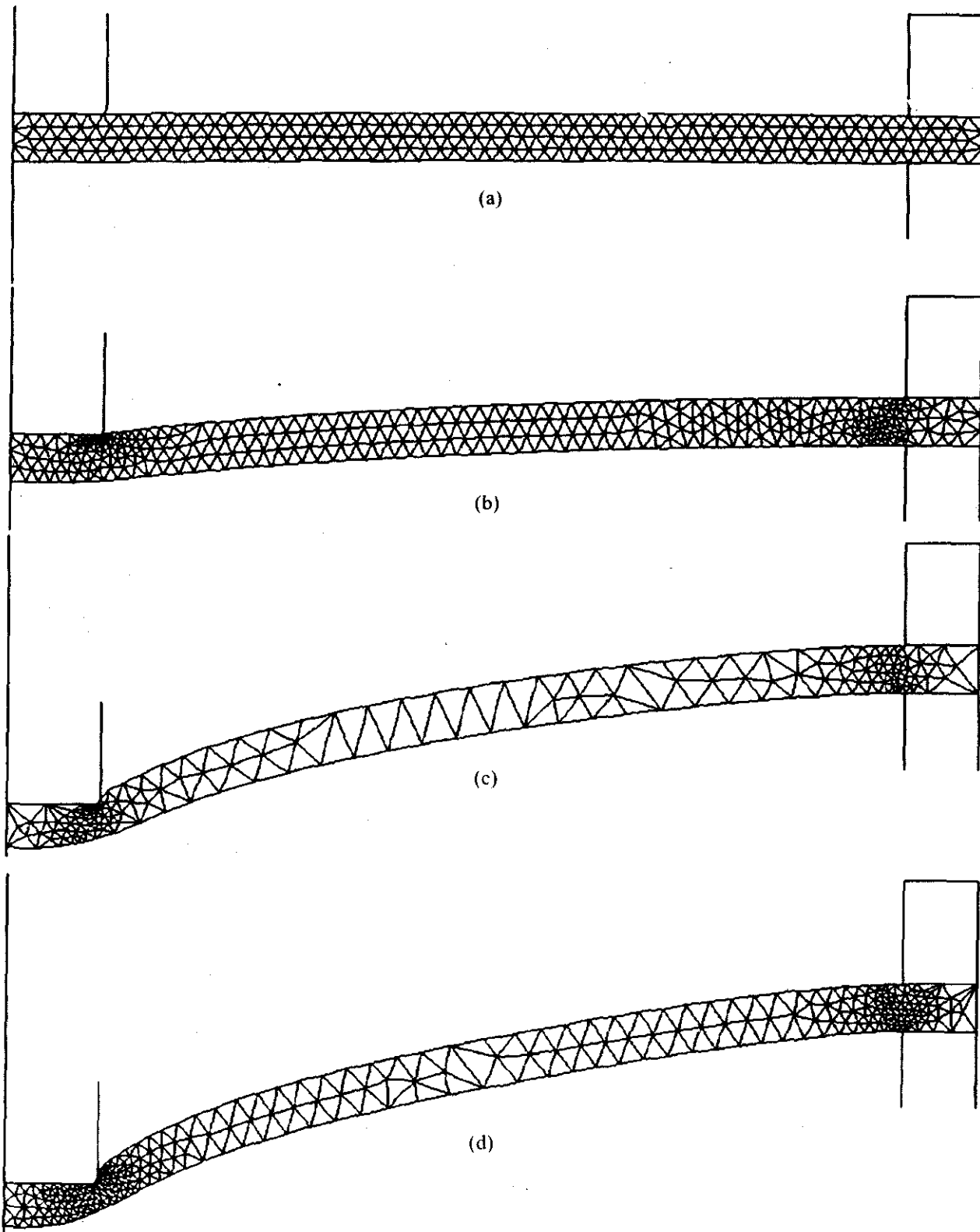


Figure 1. Progress of deformation during impact of a blunt-ended projectile impact on an aluminium plate. (a) Number of elements = 514, number of points = 1165, (b) number of elements = 593, number of points = 1346, (c) number of elements = 282, number of points = 647, (d) number of elements = 496, number of points = 1115.

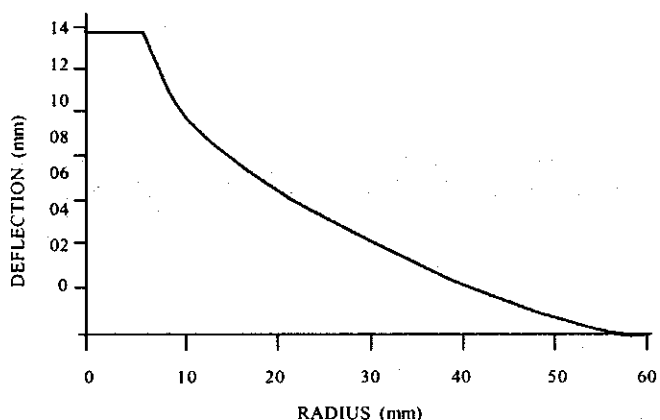


Figure 2. Final deflected profile of target plate under the impact of blunt-end projectile.

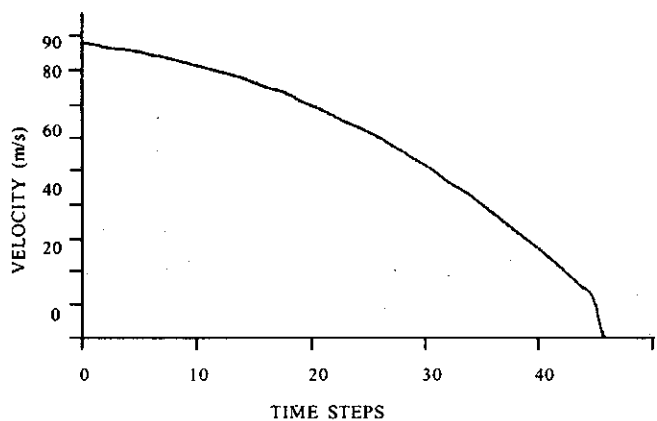


Figure 3. Variation of projectile velocity during deformation of aluminium plate under impact of blunt-end projectile.

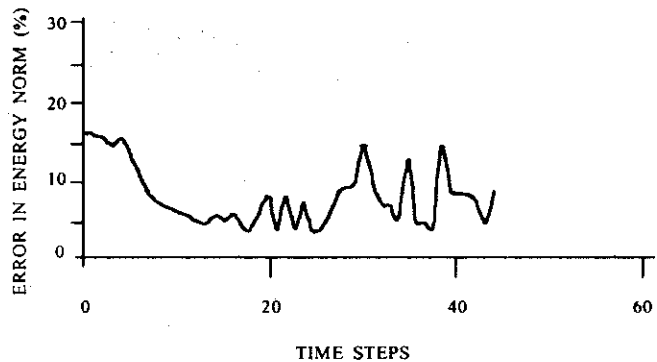


Figure 4. Error variation during deformation process of the target plate under the impact of blunt-end projectile.

### 4.2 Impact of a Thin Target by Hemispherical Head Projectile

The impact of a hemispherical-head projectile on an aluminum plate of thickness 1.27 mm and diameter 120 mm is simulated with the help of the program developed for this purpose. The constitutive model<sup>2</sup> for 2024 aluminum is given as  $\bar{\sigma} = 352\bar{\epsilon}^{-0.16}$  where  $\bar{\sigma}$  is effective stress and  $\bar{\epsilon}$  are the effective strain.

The projectile is cylindrical having diameter 12.7 mm and mass 38.4 g. It hits normally at the centre of the plate with the velocity of 33.33 m/s. The specific heat capacity of aluminum is 875 J/kg. K. and mass density 2780 kg/m<sup>3</sup>.

The values of computational parameters are as follows:  $\eta_u$  (upper limit of error) = 10 per cent.  $\eta_a$  (aiming error) = 9 per cent.  $\Delta t = 5$  ms. Total number of steps = 89. A somewhat higher limit  $\eta_u$  has been chosen to generate the meshes so that few more steps can be continued without regeneration. Generally  $\eta_u > \eta_a$ . Whenever the error in the solution ( $\eta$ ) exceeds  $\eta_u$ , the mesh is regenerated by taking the error limit  $\eta_a$  in the computation of new mesh size so that the error in the next step can be expected to be less than  $\eta_a$ , which is lower than  $\eta_u$ . This avoids frequent mesh regeneration. Adaptive mesh generation is visible near the region of high stress concentration, i.e., the zone of projectile impact. The local deformation near the projectile is more as compared to that at larger radii.

The deformation of the plate at different time steps is shown in Fig. 5. The deflection of the plate continues until the projectile velocity dies out. Finally, the plate at the centre takes the shape of a spherical head. The maximum deflection of the plate is found to be 10.3 mm. From Fig. 6, it is evident that the local deformation of the plate at the centre is more compared to the global deformation of the plate. The velocity variation during the impact is given in Fig. 7.

Initially, the mesh contains 835 elements and 1954 nodes. As the percentage error ( $\eta$ ) in the energy norm is more than the pre-defined error limit, (Fig. 8), mesh is regenerated. It increases

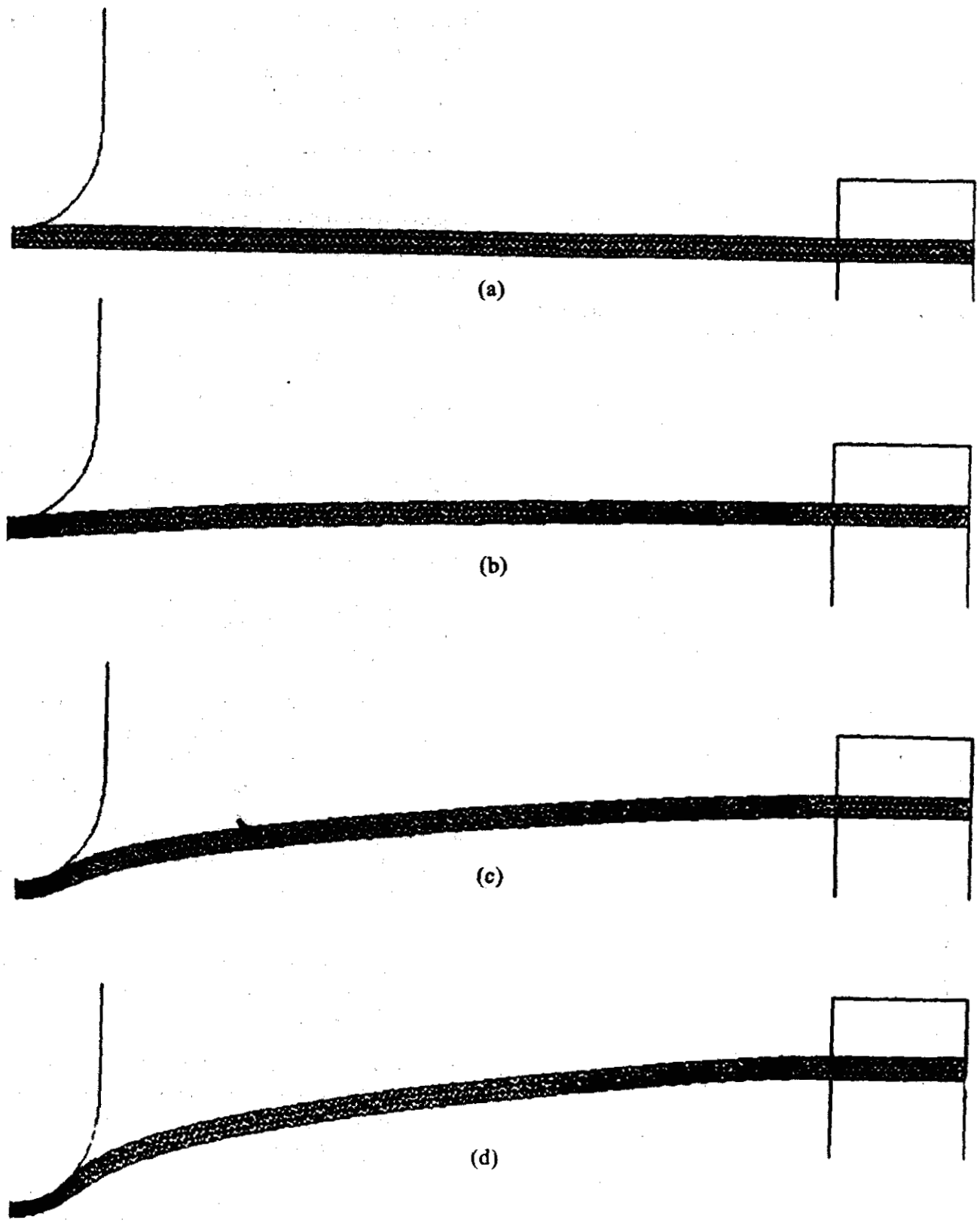


Figure 5. Progress of deformation during impact of a hemispherical-head projectile on an aluminium plate. (a) Initial mesh, (b) mesh at time step = 11, (c) mesh at the time step = 40, and (d) mesh at time step = 89.

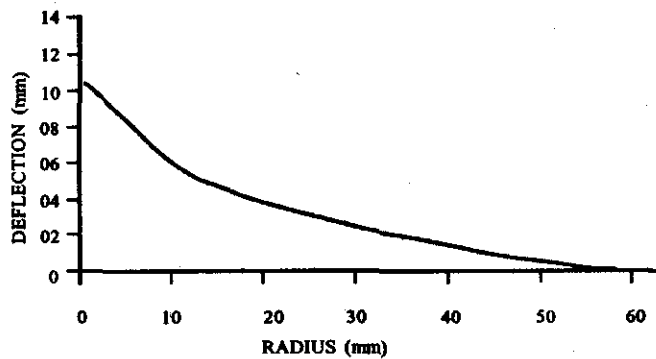


Figure 6. Final deflected profile of target plate under the impact of spherical-head projectile.

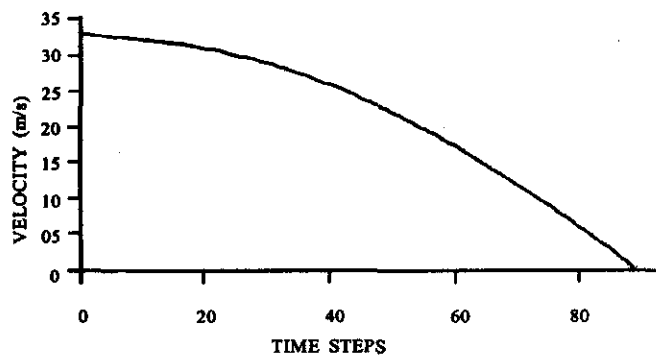


Figure 7. Variation of projectile velocity during deformation of aluminium plate under the impact of hemispherical-head projectile.

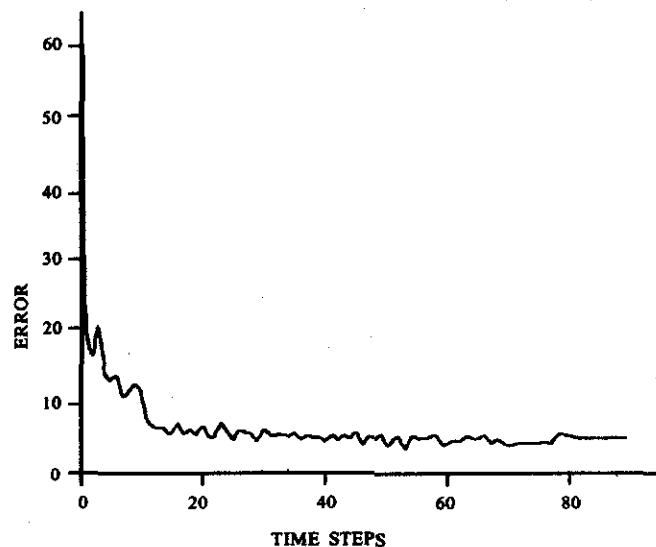


Figure 8. Error variation during the deformation process under the impact of hemispherical-head projectile.

the number of elements and nodes to be 1371 and 3094, respectively. In the remaining time steps, the error is found to be around 5 to 6 per cent which is well below the error limit.

## 5. CONCLUSION

The finite-element method for the flow formulation coupled with the error estimator captures the high stress-strain gradient zone and refines the zone automatically to minimise the error in the solution. From the illustrated problems, it is evident that this method improves the solution and simulates the impact phenomenon accurately.

## ACKNOWLEDGEMENT

The authors wish to express their gratitude to the Armament Research Board (ARMREB) for financial help for the present study.

## REFERENCES

- 1 Backman, M. E. & Goldsmith, W. The mechanics of penetration of projectiles into targets. *Inter. J. Engg. Sci.*, 1978, 16, 1-99.
- 2 Levy, N. & Goldsmith, W. Normal impact and perforation of thin plates by hemi-spherically tipped projectiles - II, Experimental Results. *Inter. J. Impact Engg.*, 1984, 2, 229-24.
- 3 Liss, Joshua & Goldsmith, Werner. Plate perforation phenomenon due to normal impact by blunt cylinders. *Inter. J. Impact Engg.*, 1984, 2, 37-64.
- 4 Kobayashi, Shiro; Oh, Soo-ik & Altan, Taylan. Metal forming and the finite-element method. 1989, Oxford University Press, UK.
- 5 Zienkiewicz, O.C.; Taylor, R.L. & Too, J.M. Reduced integration technique in general analysis of plates and shells. *Inter. J. Num. Meth. Engg.*, 1971, 3, 275-90.
- 6 Coupez, T. & Chenot, J.L. A new approach for enforcing the incompressibility in the finite-element visco-plastic flow formulation. *In Computational plasticity: models, software and*